A pilot study to establish an ovalbumin-induced atopic dermatitis minipig model

Young Kyu Kim, Ju Young Lee, Jeong Ho Hwang[✉], Han Na Suh[✉]

Animal Model Research Group, Korea Institute of Toxicology,
30 Baekhak1-gil, Jeongeup, Jellabuk-do, 56212, Republic of Korea
jeongho.hwang@kitox.re.kr; hanna.suh@kitox.re.kr

Abstract

Introduction: Because minipig skin is similar to human skin in anatomy and physiology, establishing an atopic dermatitis (AD) minipig model seems meaningful. **Material and Methods:** We applied 1-fluoro-2,4-dinitrobenzene (DNFB) or ovalbumin onto the back skin of five Yucatan minipigs aged 8–10 months and 19 kg in median weight. Two minipigs with the same parameters served as controls. **Results:** Both DNFB and ovalbumin mediated epithelial hyperplasia, spongiosis, and immune cell infiltration in the dermis, which is a typical histopathological feature of AD. Moreover, AD upregulated the Th1- and Th2-related cytokine expressions in DNFB- or in ovalbumin-treated skin. Notably, AD-induced minipigs exhibited greater cytokine serum concentrations. **Conclusion:** Histopathological finding and cytokine analysis revealed that DNFB or ovalbumin mediates AD. However, ovalbumin-treated minipig is a more reliable and precise AD model owing to the DNFB-induced severe skin damage. In summary, ovalbumin-treated skin shows similar AD as human in histopathological and molecular analysis.

Keywords: atopic dermatitis, Yucatan minipig, 1-fluoro-2,4-dinitrobenzene, ovalbumin.

Introduction

Skin is a physical barrier preventing water loss and protecting against penetration by external organisms (9). Atopic dermatitis (AD) is an inflammatory skin disorder that presents with pruritus, erythema, swelling, dryness, and fissures. It affects approximately 20% of all people at least once in their lifetime, more commonly in childhood (24, 33). A defect of epidermal integrity due to AD facilitates allergen or hapten entry into the skin and triggers an immune response (20). As AD has complex aetiology involving immune system disorders and/or overactivity, the treatment approach is mainly focused on symptom relief. Recently, a monoclonal antibody against a specific target protein has emerged as another therapeutic option along with the use of conventional drugs (7). Single treatment with lokivetmab, the anti-interleukin 31 (IL-31) antibody is an effective treatment to attenuate pruritus in dogs (30, 32, 39, 41–43). Precise methods to test the safety and efficacy of new drugs are essential and among them animal models play a significant role in developing novel diagnostic tools and drugs. They are also useful in understanding disease pathogenesis and in the specific case of AD an animal model has both utilities.

The Nc/Nga mouse has been identified as a spontaneous AD animal model (27), which have established by several researchers.

Epicutaneous sensitisation with allergens (20, 40) or haptens (26, 28) has been widely used to establish an AD or allergic contact dermatitis (ACD) model. House dust mites and allergens such as ovalbumin evoke a Th2-dominated response (15, 16). However, haptens such as oxazolone, 2,4-dinitrofluorobenzene (DNFB), or 2,4,6-trinitrochlorobenzene (TNCB), mediates the Th1 response (28). Another AD animal model can be established through overexpression of cytokine genes *e.g. interleukin 4* (*IL-4*) and *IL-31* (6, 8). Considering the cost-effectiveness and the lesser labour demand with animal models exploiting rodents, researchers favour such. However, rodent skin is different to human skin in terms of anatomy and physiology (22, 23), and differences in drug permeability and local immune reactions between the two are unavoidable. Therefore, a more reliable AD animal model similar to human is required.

Porcine skin is composed of an epidermis, dermis, and tightly connected subcutaneous layer. The thickness of the epidermis is 30–140 μm in pigs, while it is 50–120 μm in humans (13, 25). In addition, the

thickness ratio of epidermis-dermis is approximately 1:10 to 1:13 in pigs, which is similar to that in humans (29). Moreover, the blood vessel and nerve distribution in the dermis are comparable with those in humans (45). These numerous similarities make the porcine a superior model for studies of skin wound healing (2, 17), burns (1), transdermal drug delivery (3, 11), and ACD (44). Thus, we selected the Yucatan minipig to establish the required AD animal model. In this study, we compared the known DNFB-induced AD with a novel ovalbumin-induced AD minipig model. Gross observation, histopathology, and cytokine analysis indicated that ovalbumin is more reliable AD model.

Material and Methods

Animals, husbandry, and feeding. Seven specific pathogen–free Yucatan minipigs, (*Sus Scrofa*) aged 8–10 months and weighing 15.05–21.17 kg (median weight 18.97 kg) were supplied from Optipharm (Osong, South Korea). They were transported in filter boxes and acclimatised for 7 days in the minipig facility at the Korea Institute of Toxicology. The experimental and control animals were housed individually in a perforated-bottom cage (850mm × 895mm × 845mm) without bedding. Room temperature and humidity were regulated in respective 19–27°C and 30–70% ranges. Fluorescent lighting of 300–700 Lux and air changes 10–20 times/h were maintained. Water was provided *ad libitum* and feed (PurinaMills, Gray Summit, MO, USA) was provided at the rate of 2% of the body weight per day. All the animal experiments were conducted under the Institutional Animal Care and Use Committee guideline of the Korea Institute of Toxicology (IACUC approval nos 20-1-0071 and 20-1-0158).

Experimental procedure. The experiment was performed from March to June 2020. To establish the AD minipig model, the experimental animals were administered xylazine (0.7 mg/kg, IM; Bayer, Leverkusen, Germany) and ketamine (20 mg/kg, IM; Yuhan Corporation, Seoul, Korea) mixture as an anaesthetic, then the back skin was shaved with clippers, sterilised with 70% isopropyl alcohol, and DNFB or ovalbumin was applied using Tegaderm™ (cat no. 3584; 3M, St. Paul, MN, USA). For DNFB treatment, the minipigs were sensitised with 1 mL of 10% DNFB dissolved in acetone:dimethyl sulphoxide (DMSO):olive oil (5:1:3, v/v/v) for 24 h (one individual) or 30 min (two individuals) on day 1, and next were challenged with 1 mL of 1% DNFB dissolved in acetone:olive oil (8:1.9, v/v) for 2 h on day 15. For ovalbumin treatment, two minipigs were sensitised with 1 mg ovalbumin dissolved in normal saline for 16 days. The remaining two minipigs served as controls. For gross observation, macroscopic images were acquired on days 3, 8, 10, 15, and 17. On day 18, minipigs were euthanised by pentobarbital sodium (100 mg/kg, IV; JW Pharmaceutical, Seoul, South Korea) and skin tissue samples from all four quadrants of the treated area were obtained using a 5 mm biopsy punch for histology and molecular analyses and blood samples (10 mL) were obtained for serum cytokine analysis.

Masson's trichrome staining. Masson's trichrome staining was performed following the manufacturer's protocol (cat no. IFU-2; ScyTek, Logan, UT, USA). Deparaffinised slides were incubated with Weigert's iron haematoxylin, solutions of Biebrich scarlet-acid fuchsin, phosphomolybdic-phosphotungstic acid, and finally aniline blue. Then, the slides were rinsed with 1% acetic acid solution. The collagen connective tissues were stained blue, nuclei were stained dark red/purple, and cytoplasm was stained red/pink.

Immunohistochemistry (IHC). The skin tissues were fixed in 10% neutral buffered formalin overnight and then embedded in paraffin. Then, the tissue samples were sectioned at 5 μm, deparaffinised, processed for antigen retrieval, blocked, and finally incubated with the primary and peroxidase-conjugated secondary antibodies. For the peroxidase-conjugated secondary antibody, 3,3′-diaminobenzidine (DAB) substrate was used followed by haematoxylin for nuclear counterstaining. Primary antibodies against CD4 (cat. no. MA5-12259; 1:5 dilution; Invitrogen, part of Thermo Fisher Scientific, Waltham, MA, USA), major basic protein (MBP; cat. no. NBP 1-42104; 1:10 dilution; Novus Biologicals, Centennial, CO, USA), and CD11b (cat. no. ab34216; 1:10 dilution; Abcam, Cambridge, UK) were used. The samples were mounted on slides and photographed with an AxioCam microscope camera, and the images were analysed with AxioVision software (both Zeiss, Oberkochen, Germany).

Quantitative reverse transcription-polymerase chain reaction (qRT-PCR). For gene expression analysis, the skin tissues were processed for RNA extraction with an RNeasy Mini Kit (Qiagen, Hilden, Germany) and reverse transcription with iScript RT Supermix for RT-qPCR (Biorad, Hercules, CA, USA). Glyceraldehyde-3-phosphate dehydrogenase was used as an endogenous control for normalisation. The quantitative chain reaction was performed with intron-spanning primers, the sequences of which are listed in Table 1. Fold induction was quantified using the $2^{-\Delta\Delta CT}$ method.

Enzyme-linked immunosorbent assay (ELISA). To analyse the cytokines in the skin, samples were homogenised in 200 μL ice-cold phosphate-buffered saline and centrifuged at 13,000 rpm for 10 min at 4°C. Then, the supernatant was obtained. To analyse the cytokines in the blood, whole blood was collected into a conical tube and allowed to clot for 30 min at room temperature. Then, it was centrifuged for 10 min at 3,000 rpm, and the supernatant was collected as serum. Porcine interleukin 4 (IL-4), interferon gamma (IFNγ) and interleukin 13 (IL-13) were measured by ELISAs (cat. nos DY654 and 985; DuoSet ELISA, R&D Systems, Minneapolis, MN, USA for IL-4 and IFNγ; and cat. no. ESIL13 for IL-13; Invitrogen) according to the manufacturer's protocols.

Statistical analyses. Student's *t*-test was used for comparisons of two samples. P values < 0.05 were considered significant. Two biological replicates and three experimental replicates were carried out.

Results

DNFB-induced ACD minipig model. DNFB, a hapten, was used to characterise the ACD in minipigs (44). To determine whether AD had been established under DNFB-treatment conditions, we performed macroscopic and microscopic analyses. The test sites demonstrated severe skin damage on gross observation. Skin erosion and ulceration with mild exudate were observed and remained scabbing was found (Fig. 1A). In histopathological analysis, the epidermis showed diffuse hyperplasia (acanthosis) and intracellular oedema of the epithelial cells (spongiosis). Moreover, perivascular immune cell infiltration was observed at the epidermis–dermis junction (Fig. 1B). To clarify which immune cells were deposited, immunohistochemistry was performed for identification of CD4, MBP, and CD11b. Notably, all three types of immune cells, *i.e.* CD4+ T lymphocytes, MBP+ eosinophils, and CD11b+ macrophages were observed at the epidermis–dermis junction (Fig. 1C). We observed that 10% DNFB treatment for 24 h disrupted of the skin barrier, damaged cells in the epidermis, and facilitated immune cell infiltration into the dermis. The skin damage was extremely severe, unlike that in human AD. Thus, we modified the experimental protocol and conducted the experiments again.

After the shorter, 30 min sensitisation, the outer layer of the skin was found to be swollen and red and a crust had formed over it (days 3–10). However, the severity was less than that exhibited by the minipigs which had been sensitised for 24 h (Fig. 1A). From the challenge, scabbing remained constant with no phenotypic difference from day 15 to day 17 (Fig. 2A). In Masson's trichrome staining, an increase in the epidermis thickness (acanthosis) when compared with that of the untreated skin, spongiosis of the epidermis, and moderate immune cell infiltration in the dermis were observed (Fig. 2B and 2C). In immunohistochemistry, the counts of CD4+ lymphocytes and MBP+ eosinophils were massively increased, while CD11b+ macrophages were not detected (Fig. 2D–2F). These data suggest that 30 min treatment with 10% DNFB inflicts more similar AD to the human variety than 24 h treatment in terms of gross observation and histological findings. However, it may not be a suitable AD model due to skin layer damage. Another ligand was applied to develop an AD minipig model without this problematic aspect.

Ovalbumin-induced AD minipig model. Ovalbumin-induced AD provoked a dominant Th2 response like human AD (16). It was noted that ovalbumin-treated sites gradually developed redness and hyperkeratosis. Scabs or exudate were not detected (Fig. 3A). However, ovalbumin also mediated acanthosis, spongiosis, and mild immune cell infiltration (Fig. 3B and 3C). Infiltrated immune cells in the skin were identified as CD4+ lymphocytes or eosinophils (Fig. 3D and 3F). These results suggested that ovalbumin induces AD, indicating similarity to human AD without any skin barrier abnormality.
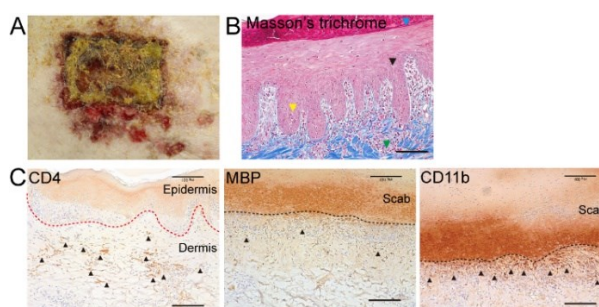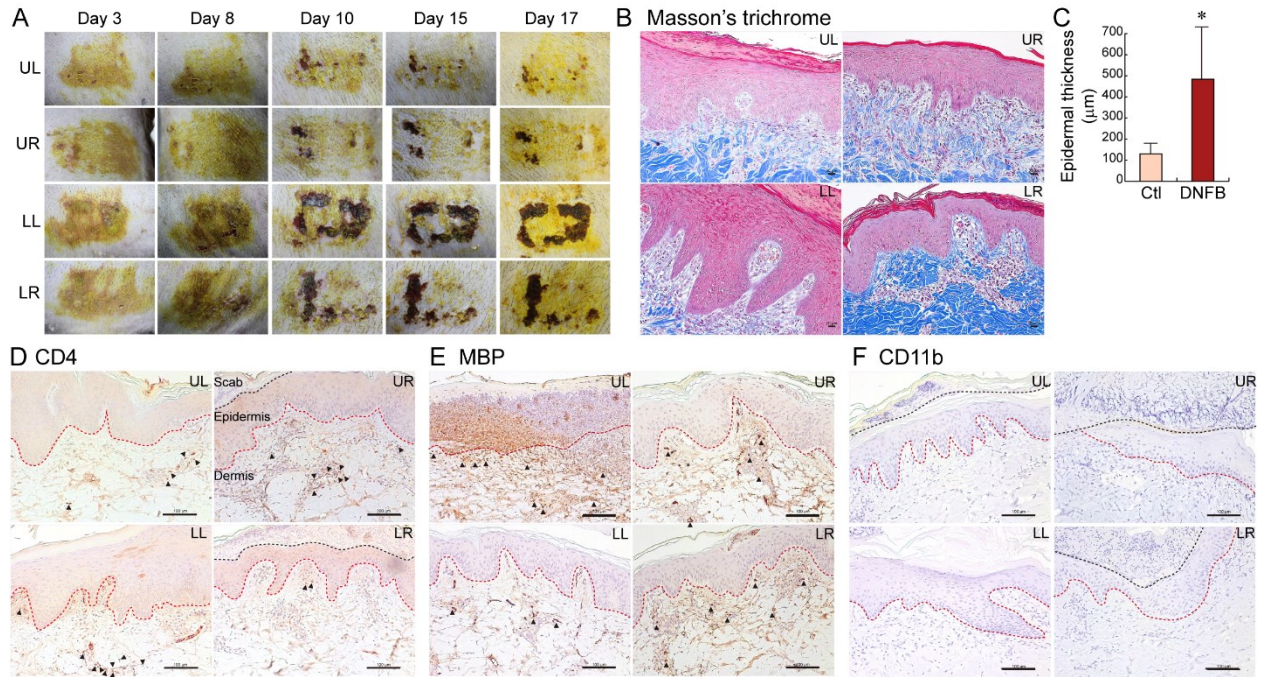

Fig. 1. Macroscopic and microscopic analysis of 1-fluoro-2,4-dinitrobenzene-induced ACD after 24h sensitisation with a 10% solution and 2h challenge with a 1% solution, shown in images which best represent the changes, selected from images of four skin tissue samples from one minipig
A – Macroscopic images of day-17 skin samples; B – Histopathological image with Masson's trichrome staining. Spongiosis is marked with a yellow arrowhead; acanthosis is marked with a black arrowhead; perivascular immune cell infiltration at the epidermis–dermis junction is marked with a blue arrowhead; C – Immunohistochemistry. CD4+ lymphocytes, major basic protein (MBP)+ eosinophils, and CD11b+ macrophages are marked by black arrow heads. Scale bar = 100 μm

Table 1. Primers used for quantitative real-time PCR

Gene symbol	Primer sequences (from 5′ to 3′)	Length	GenBank accession number
IL-4	F: GTCTGCTTACTGGCATGTACCA	118	NM214123.1
	R: GCTCCATGCACGAGTTCTTTCT		
IFNγ	F: CGATCCTAAAGGACTATTTTAATGCAA	102	NM213948.1
	R: TTTTGTCACTCTCCTCTTTCCAAT		
IL-13	F: GGATGATTTTTCGCCACGGG	78	NM213803.1
	R: ATGGTAAAGGGCTGCCTCTG		
GAPDH	F: ACAGACAGCCGTGTGTTCC	60	NM001206359.1
	R: ACCTTCACCATCGTGTCTCA		

IL-4 – interleukin 4; *IFNγ* – interferon gamma; *IL-13* – interleukin 13; *GAPDH* – glyceraldehyde-3-phosphate dehydrogenase

Fig. 2. Macroscopic and microscopic analysis of modified 1-fluoro-2,4-dinitrobenzene-induced ACD after 30 min sensitisation with a 10% solution and 2h challenge with a 1% solution shown in images which best represent the changes, selected from images of eight skin tissue samples from two minipigs

A – Macroscopic images of day-3, day-8, day-10, day-15, and day-17 skin samples; B – Histopathological image with Masson's trichrome staining. Scale bar = 20 μm; C – Thickness of epidermis. p* < 0.05; D–F – Immunohistochemistry. D – CD4+ lymphocytes; E – major basic protein (MBP) + eosinophils; F – CD11b+ macrophages. All named cells are marked by black arrowheads. Margins of scab, epidermis, and dermis are marked with dotted lines. Scale bar = 100 μm; Ctl – controls; DNFB – 1-fluoro-2,4-dinitrobenzene; UL – upper left; UR – upper right; LL – lower left; LR – lower right
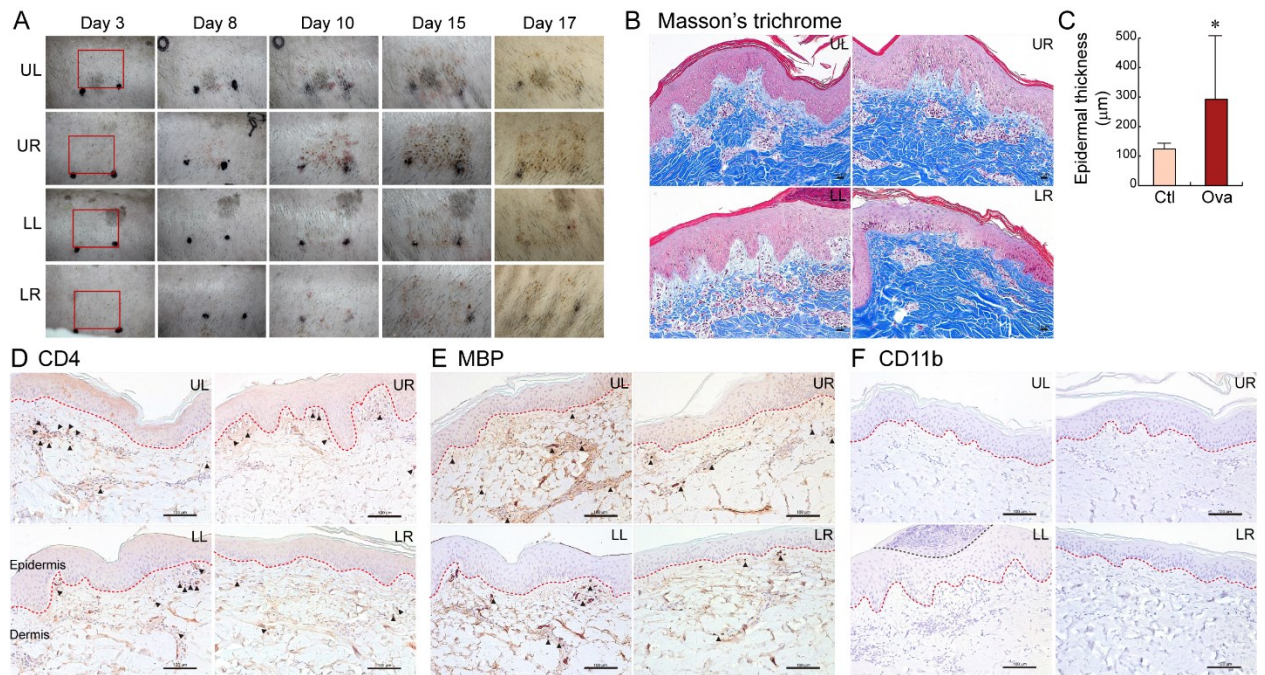

Fig. 3. Macroscopic and microscopic analysis of ovalbumin-induced AD shown in representative images shown in images which best represent the changes, selected from images of eight skin tissue samples from two minipigs

A – Macroscopic images of day-3, day-8, day-10, day-15, and day-17 skin samples; B – Histopathological image with Masson's trichrome staining. Scale bar = 20 μm; C – Thickness of epidermis. p* < 0.05; D–F – Immunohistochemistry. D – CD4+ lymphocytes; E – major basic protein (MBP) + eosinophils; F – CD11b+ macrophages. All named cells are marked by black arrowheads. Margins of scab, epidermis, and dermis are marked with dotted lines. Scale bar = 100 μm; Ctl – controls; ova – ovalbumin; UL – upper left; UR – upper right; LL – lower left; LR – lower right
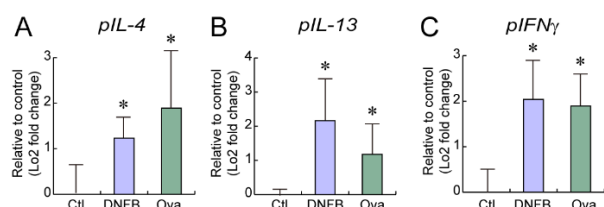
Fig. 4. Analysis of the cytokine mRNA in AD skin as quantified by quantitative reverse transcriptase PCR
A – porcine (*p*) *IL-4*; B – porcine *IL-13*; C –porcine *IFNγ*. Ctl – controls; DNFB – 1-fluoro-2,4-dinitrobenzene; Ova – ovalbumin. Values are mean ± SD. *p < 0.05
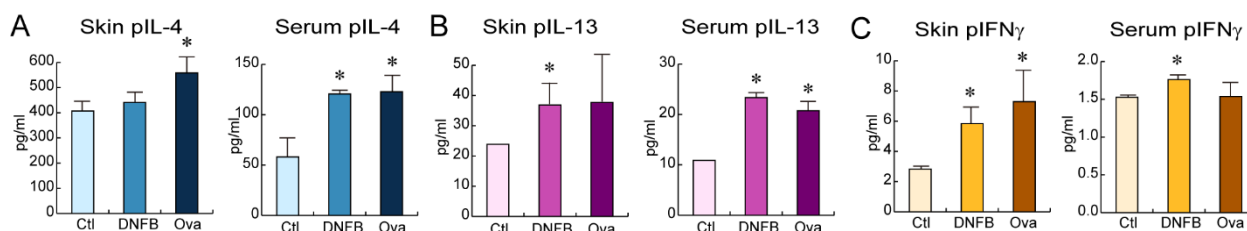
Fig. 5. Analysis of the absolute cytokine protein level in AD skin and serum as quantified by ELISA
A – porcine (*p*) IL-4; B – porcine IL-13; C –porcine IFNγ. Ctl – controls; DNFB – 1-fluoro-2,4-dinitrobenzene; Ova – ovalbumin. Values are mean ± SD. *p < 0.05

Analysis of cytokines in the skin and serum of subjects with induced AD. To determine which cytokines were regulated by DNFB or ovalbumin, we analysed the cytokines in the skin and serum samples. We detected an increase in the counts of CD4+ lymphocytes and eosinophils under DNFB or ovalbumin treatment, which suggests the upregulation of the cytokines (Figs 2 and 3). The cytokine mRNA expression levels of *IL-4*, *IL-13*, and *IFNγ* as well as the absolute levels of IL-4, IL-13, and IFNγ were found to be enhanced in both DNFB- and ovalbumin-induced dermatitic minipig skin (Figs 4A–4C and 5A–5C). Interestingly, we also noted that the cytokine levels had increased in the serum sample, indicating a strong relationship between local inflammation and systemic inflammation (Fig. 5A–5C). Although these cytokines were related to the Th1 or Th2 immune response, we found that DNFB and ovalbumin-induced AD upregulated all three cytokine levels in the skin and serum samples.

Discussion

In this study, we developed an AD minipig model by applying DNFB and ovalbumin ligands with 24 h or 30 min treatment times. As AD is diagnosed based on the symptoms of skin inflammation (such as pruritus, erythema, and hyperkeratosis), the potential for similar gross observations in an animal model as in human AD is essential. The minipig is the only experimental animal that has tight subcutaneous connective tissue and similar thickness of the skin layer to humans. Thus, this species were chosen to establish the AD animal model. Sensitisation only with DNFB had been used to develop an AD minipig model prior to this research (44). DNFB triggers the formation of Langerhans or dendritic cells in the dermis when it induces AD, and these cells migrate to the lymph node and then prime naïve T cells. When the skin is re-exposed to DNFB, allergen-specific CD8+ T cell-mediated skin inflammation occurs (10). However, DNFB in a solvent (acetone:DMSO:olive oil mixture) seems to damage the skin severely. Regardless of the DNFB treatment duration being short or long, DNFB-applied skin was affected by physical disruption of the skin barrier (Figs 1A and 2A). Ovalbumin-induced AD involves different pathological mechanisms to the DNFB-induced condition. Ovalbumin-sensitised skin was infiltrated by more CD4+ T cells and eosinophils, and responded in the dominant-Th2 manner producing more IL-4, IL-5, and IL-13 (26, 27). As ovalbumin mainly mediates the Th2 response, we assumed that ovalbumin treatment may induce typical AD. In fact, the skin did not reveal any epithelial defect, but redness and hyperkeratosis were detected after ovalbumin treatment (Fig 3A). Furthermore, DNFB and ovalbumin increased the counts of CD4+ T lymphocytes and MBP+ eosinophils in the dermis (Figs 2D, 2E, 3D and 3E). Ovalbumin-induced AD in mice showed tissue infiltration by CD4+ T lymphocytes and CD11b+ macrophages (18), while eosinophil infiltration was found in DNFB-induced AD in the same experimental model (19). The difference in the infiltrating immune cells might be related to different species (rodent *vs*. porcine) or tissue collection time points. Although both DNFB and ovalbumin increase the immune cell infiltration, the skin damage induced by DNFB suggests that the use of ovalbumin is a method equally to be recommended for developing an AD minipig model.

It is known that DNFB or ovalbumin induce different immune responses (Th1 *vs.* Th2). However, some other studies have reported that T cell polarisation is regulated by the progression of AD. The Th2 response is dominant in acute AD, while the Th1 response is

dominant in the chronic form (5, 34). Moreover, cutaneous ovalbumin sensitisation mediates the combination of Th1, Th2, and Th17 immune responses (35). In fact, we noted that DNFB or ovalbumin upregulate both Th2-related *IL-4* and *IL-13* and Th1-related *IFNγ* with statistical significance (Fig. 4A–4C). Moreover, the absolute cytokine levels of IFNγ were upregulated in DNFB- or ovalbumin-treated skin also with statistical significance (Fig. 5C). Thus, it seems that the present AD model induced by DNFB or ovalbumin elicited combined Th2 and Th1 immune responses. Interleukins 4 and 13 upregulated collagen synthesis *via* the extracellular signal-related kinase pathway in human dermal fibroblasts (4). In addition, the skin barrier protein filaggrin was decreased by IL-4 and IL-13 (14). Interferon gamma regulates the immunological functions of epidermal keratinocytes such as leukocyte migration, immune cell-related surface marker expression, and pro-inflammatory cytokine production (12, 31, 37). Thus, our findings of increased expressions of IL-4, IL-13, and IFNγ are strongly related to epidermal thickness and immune cell infiltration.

There is evidence that AD initiates local skin inflammation, elevates cytokines levels and activates T cell, leading to a systemic inflammatory response (40). Airway inflammation (21) as well as cardiovascular and neuropsychiatric disorders (36, 38) accompanied AD. Fig. 5 demonstrates a similar cytokine expression pattern in the serum to that in the skin, indicating the possibility of systemic inflammation under DNFB or ovalbumin treatment. In the present study, the outcomes of induction of AD in minipig models by DNFB and ovalbumin were compared. Both DNFB and ovalbumin mediated epidermal hyperplasia, epidermal oedema formation, and CD4+ T lymphocyte and eosinophil infiltration into the dermis, and upregulated inflammatory cytokine expression. Interestingly, DNFB induced severe skin damage, while ovalbumin showed a similar macroscopic phenotype to that of human AD. Based on these results, we concluded that the ovalbumin-treated AD minipig is the more reliable and representative animal model. To the best of our knowledge, this is the first study utilising ovalbumin to induce AD in a minipig model. We hope that the ovalbumin-induced AD minipig model becomes a valuable tool for development of drugs to treat AD. Proven as it is by histopathological findings for phenotype and immune cell infiltration and molecular findings for cytokines, the ovalbumin-induced AD minipig model is a sufficiently representative model for this purpose in our contention.

Conflict of Interests Statement: The authors declare that there is no conflict of interests regarding the publication of this article.

References

1. Abdullahi A., Amini-Nik S., Jeschke M.G.: Animal models in burn research. Cell Mol Life Sci 2014, 71, 3241–3255, doi: 10.1007/s00018-014-1612-5.
2. Ansell D.M., Holden K.A., Hardman M.J.: Animal models of wound repair: Are they cutting it?, Exp Dermatol 2012, 21, 581–585, doi: 10.1111/j.1600-0625.2012.01540.x.
3. Barbero A.M. Frasch H.F.: Pig and guinea pig skin as surrogates for human in vitro penetration studies: a quantitative review. Toxicol In Vitro 2009, 23, 1–13, doi: 10.1016/j.tiv.2008.10.008.
4. Bhogal R.K. Bona C.A.: Regulatory effect of extracellular signal-regulated kinases (ERK) on type I collagen synthesis in human dermal fibroblasts stimulated by IL-4 and IL-13. Int Rev Immunol 2008, 27, 472–496, doi: 10.1080/08830180802430974.
5. Bieber T.: Atopic dermatitis. N Engl J Med 2008, 358, 1483–1494, doi: 10.1056/NEJMra074081.
6. Chan L.S., Robinson N., Xu L.: Expression of interleukin-4 in the epidermis of transgenic mice results in a pruritic inflammatory skin disease: an experimental animal model to study atopic dermatitis. J Invest Dermatol 2001, 117, 977–983, doi: 10.1046/j.0022-202x.2001.01484.x.
7. Del Rosso J.Q.: Monoclonal Antibody Therapies for Atopic Dermatitis: Where Are We Now in the Spectrum of Disease Management? J Clin Aesthet Dermatol 2019, 12, 39–41.
8. Dillon S.R., Sprecher C., Hammond A., Bilsborough J., Rosenfeld-Franklin M., Presnell S.R., Haugen H.S., Maurer M., Harder B., Johnston J., Bort S., Mudri S., Kuijper J.L., Bukowski T., Shea P., Dong D.L., Dasovich M., Grant F.J., Lockwood L., Levin S.D., LeCiel C., Waggie K., Day H., Topouzis S., Kramer J., Kuestner R., Chen Z., Foster D., Parrish-Novak J., Gross J.A.: Interleukin 31, a cytokine produced by activated T cells, induces dermatitis in mice. Nat Immunol 2004, 5, 752–760, doi: 10.1038/ni1084.
9. Elias P.M.: Skin barrier function. Curr Allergy Asthma Rep 2008, 8, 299–305, doi: 10.1007/s11882-008-0048-0.
10. Fukunaga A., Khaskhely N.M., Sreevidya C.S., Byrne S.N., Ullrich S.E.: Dermal dendritic cells, and not Langerhans cells, play an essential role in inducing an immune response. J Immunol 2008, 180, 3057–3064, doi: 10.4049/jimmunol.180.5.3057.
11. Godin B.,Touitou E.: Transdermal skin delivery: predictions for humans from in vivo, ex vivo and animal models. Adv Drug Deliv Rev 2007, 59, 1152–1161, doi: 10.1016/j.addr.2007.07.004.
12. Griffiths C.E., Esmann J., Fisher G.J., Voorhees J.J., Nickoloff B.J.: Differential modulation of keratinocyte intercellular adhesion molecule-I expression by gamma interferon and phorbol ester: evidence for involvement of protein kinase C signal transduction. Br J Dermatol 1990, 122, 333–42, doi: 10.1111/j.1365-2133.1990.tb08281.x.
13. Hammond S.A., Tsonis C., Sellins K., Rushlow K., Scharton-Kersten T., Colditz I., Glenn G.M.: Transcutaneous immunization of domestic animals: opportunities and challenges. Adv Drug Deliv Rev 2000, 43, 45–55, doi: 10.1016/s0169-409x(00)00076-4.
14. Howell M.D., Fairchild H.R., Kim B.E., Bin L., Boguniewicz M., Redzic J.S., Hansen K.C., Leung D.Y.: Th2 cytokines act on S100/A11 to downregulate keratinocyte differentiation. J Invest Dermatol 2008, 128, 2248–2258, doi: 10.1038/jid.2008.74.
15. Huang C.H., Kuo I.C., Xu H., Lee Y.S., Chua K.Y.: Mite allergen induces allergic dermatitis with concomitant neurogenic inflammation in mouse. J Invest Dermatol 2003, 121, 289–293, doi: 10.1046/j.1523-1747.2003.12356.x.

16. Jin H., He R., Oyoshi M., Geha R.S.: Animal models of atopic dermatitis. J Invest Dermatol 2009, 129, 31–40, doi: 10.1038/jid.2008.106.

17. Jung Y., Son D., Kwon S., Kim J., Han K.: Experimental pig model of clinically relevant wound healing delay by intrinsic factors. Int Wound J 2013, 10, 295–305, doi: 10.1111/j.1742-481X.2012.00976.x.

18. Kim B.E., Leung D.Y.M.: Significance of Skin Barrier Dysfunction in Atopic Dermatitis. Allergy Asthma Immunol Res 2018, 10, 207–215, doi: 10.4168/aair.2018.10.3.207.

19. Kim G.-D., Kim T.-H., Park Y.-S., Ahn H.-J., Cho J.-J., Park C.-S.: Immune response against 2,4-dinitrofluorobenzene-induced atopic dermatitis-like clinical manifestation is suppressed by spermidine in NC/Nga mice. Scand J Immunol 2015, 81, 221–228, doi: 10.1111/sji.12274.

20. Kimura M., Tsuruta S., Yoshida T.: Correlation of house dust mite-specific lymphocyte proliferation with IL-5 production, eosinophilia, and the severity of symptoms in infants with atopic dermatitis. J Allergy Clin Immunol 1998, 101, 84–89, doi: 10.1016/S0091-6749(98)70197-6.

21. Kubo A., Nagao K., Amagai M.: Epidermal barrier dysfunction and cutaneous sensitization in atopic diseases. J Clin Invest 2012, 122, 440–447, doi: 10.1172/JCI57416.

22. Kurihara-Bergstrom T., Woodworth M., Feisullin S., Beall P.: Characterization of the Yucatan miniature pig skin and small intestine for pharmaceutical applications. Lab Anim Sci 1986, 36, 396–399.

23. Lavker R.M., Dong G., Zheng P.S., Murphy G.F.: Hairless micropig skin. A novel model for studies of cutaneous biology. Am J Pathol 1991, 138, 687–697.

24. Leung D.Y., Bieber T.: Atopic dermatitis. Lancet 2003, 361, 151–160, doi: 10.1016/S0140-6736(03)12193-9.

25. Mahl J.A., Vogel B.E., Court M., Kolopp M., Roman D., Nogués V.: The minipig in dermatotoxicology: methods and challenges. Exp Toxicol Pathol 2006, 57, 341–345, doi: 10.1016/j.etp.2006.03.004.

26. Man M.Q., Hatano Y., Lee S.H., Man M., Chang S., Feingold K.R., Leung D.Y., Holleran W., Uchida Y., Elias P.M.: Characterization of a hapten-induced, murine model with multiple features of atopic dermatitis: structural, immunologic, and biochemical changes following single versus multiple oxazolone challenges. J Invest Dermatol 2008, 128, 79–86, doi: 10.1038/sj.jid.5701011.

27. Matsuda H., Watanabe N., Geba G.P., Sperl J., Tsudzuki M., Hiroi J., Matsumoto M., Ushio H., Saito S., Askenase P.W., Ra C.: Development of atopic dermatitis-like skin lesion with IgE hyperproduction in NC/Nga mice. Int Immunol 1997, 9, 461–466, doi: 10.1093/intimm/9.3.461.

28. Matsumoto K., Mizukoshi K., Oyobikawa M., Ohshima H., Tagami H.: Establishment of an atopic dermatitis-like skin model in a hairless mouse by repeated elicitation of contact hypersensitivity that enables to conduct functional analyses of the stratum corneum with various non-invasive biophysical instruments. Skin Res Technol 2004, 10, 122–129, doi: 10.1111/j.1600-0846.2004.00062.x.

29. Meyer W., Schwarz R., Neurand K.: The skin of domestic mammals as a model for the human skin, with special reference to the domestic pig. Curr Probl Dermatol 1978, 7, 39–52, doi: 10.1159/000401274.

30. Michels G.M., Walsh K.F., Kryda K.A., Mahabir S.P., Walters R.R., Hoevers J.D., Martinon O.M.: A blinded, randomized, placebo-controlled trial of the safety of lokivetmab (ZTS-00103289), a caninized anti-canine IL-31 monoclonal antibody in client-owned dogs with atopic dermatitis. Vet Dermatol 2016, 27, 505–e136, doi: 10.1111/vde.12364.

31. Mori T., Kabashima K., Yoshiki R., Sugita K., Shiraishi N., Onoue A., Kuroda E., Kobayashi M., Yamashita U., Tokura Y.: Cutaneous hypersensitivities to hapten are controlled by IFN-gamma-upregulated keratinocyte Th1 chemokines and IFN-gamma-downregulated langerhans cell Th2 chemokines. J Invest Dermatol 2008, 128, 1719–1727, doi: 10.1038/jid.2008.5.

32. Moyaert H., Van Brussel L., Borowski S., Escalada M., Mahabir S.P., Walters R.R., Stegemann M.R.: A blinded, randomized clinical trial evaluating the efficacy and safety of lokivetmab compared to ciclosporin in client-owned dogs with atopic dermatitis. Vet Dermatol 2017, 28, 593–e145, doi: 10.1111/vde.12478.

33. Novak N., Bieber T., Leung D.Y.: Immune mechanisms leading to atopic dermatitis. J Allergy Clin Immunol 2003, 112, S128–139, doi: 10.1016/j.jaci.2003.09.032.

34. Oyoshi M.K., He R., Kumar L., Yoon J., Geha R.S.: Cellular and molecular mechanisms in atopic dermatitis. Adv Immunol 2009, 102, 135–226, doi: 10.1016/S0065-2776(09)01203-6.

35. Oyoshi M.K., Murphy G.F., Geha R.S.: Filaggrin-deficient mice exhibit TH17-dominated skin inflammation and permissiveness to epicutaneous sensitization with protein antigen. J Allergy Clin Immunol 2009, 124, 485–493, 493.e1, doi: 10.1016/j.jaci.2009.05.042v.

36. Paller A., Jaworski J.C., Simpson E.L., Boguniewicz M., Russell J.J., Block J.K., Tofte S., Dunn J.D., Feldman S.R., Clark A.R., Schwartz G., Eichenfield L.F.: Major Comorbidities of Atopic Dermatitis: Beyond Allergic Disorders. Am J Clin Dermatol 2018, 19, 821–838, doi: 10.1007/s40257-018-0383-4.

37. Pastore S., Corinti S., La Placa M., Didona B., Girolomoni G.: Interferon-gamma promotes exaggerated cytokine production in keratinocytes cultured from patients with atopic dermatitis. J Allergy Clin Immunol 1998, 101, 538–544, doi: 10.1016/S0091-6749(98)70361-6.

38. Silverberg J.I.: Association between adult atopic dermatitis, cardiovascular disease, and increased heart attacks in three population-based studies. Allergy 2015, 70, 1300–1308, doi: 10.1111/all.12685.

39. Souza C.P., Rosychuk R.A.W., Contreras E.T., Schissler J.R., Simpson A.C.: A retrospective analysis of the use of lokivetmab in the management of allergic pruritus in a referral population of 135 dogs in the western USA. Vet Dermatol 2018, 29, 489–e164, doi: 10.1111/vde.12682.

40. Spergel J.M., Mizoguchi E., Brewer J.P., Martin T.R., Bhan A.K., Geha R.S.: Epicutaneous sensitization with protein antigen induces localized allergic dermatitis and hyperresponsiveness to methacholine after single exposure to aerosolized antigen in mice. J Clin Invest 1998, 101, 1614–1622, doi: 10.1172/JCI1647.

41. Szczepanik M.P., Popiel J., Cekiera A., Pomorska-Handwerker D., Karaś-Tęcza J., Ściskalska M., Oczkowska K., Taube M., Olender V., Parys P.: Evaluation of the clinical efficiency of lokivetmab in client privately owned atopic dogs - multicenter study. Pol J Vet Sci 2020, 23, 191–195, doi: 10.24425/pjvs.2020.132765.

42. Szczepanik M.P., Wikolek P., Goynski M., Sitkowski W., Taszkun I., Toczek W.: The influence of treatment with lokivetmab on transepidermal water loss (TEWL) in dogs with spontaneously occurring atopic dermatitis. Vet Dermatol 2019, 30, 330–e93, doi: 10.1111/vde.12758.

43. Tamamoto-Mochizuki C., Paps J.S., Olivry T.: Proactive maintenance therapy of canine atopic dermatitis with the anti-IL-31 lokivetmab. Can a monoclonal antibody blocking a single cytokine prevent allergy flares?, Vet Dermatol 2019, 30, 98, doi: 10.1111/vde.12715.

44. Vana G., Meingassner J.G.: Morphologic and immunohistochemical features of experimentally induced allergic contact dermatitis in Göttingen minipigs. Vet Pathol 2000, 37, 565–580, doi: 10.1354/vp.37-6-565.

45. Vardaxis N.J., Brans T.A., Boon M.E., Kreis R.W., Marres L.M.: Confocal laser scanning microscopy of porcine skin: implications for human wound healing studies. J Anat 1997, 190, 601–611, doi: 10.1046/j.1469-7580.1997.19040601.x.